Journal of Materials Chemistry C

Terpyridine-modified chrysene derivatives as electron transporters to improve lifetime in phosphorescent OLEDs

Journal:	*Journal of Materials Chemistry C*
Manuscript ID	TC-ART-11-2019-006393.R3
Article Type:	Paper
Date Submitted by the Author:	20-Jan-2020
Complete List of Authors:	Owada, Tsukasa; Yamagata univ., Organic Device Engineering Sasabe, Hisahiro; Yamagata univ., Organic Device Engineering Sukegawa, Yoshihito; Yamagata univ., Organic Device Engineering Watanabe, Taiki; Yamagata univ., Organic Device Engineering Maruyama, Tomohiro; Yamagata univ., Organic Device Engineering Watanabe, Yuichiro; Yamagata univ., Organic Device Engineering Yokoyama, Daisuke; Yamagata University, Department of Organic Device Engineering, Graduate School of Science and Engineering Kido, Junji; Yamagata univ., Organic Device Engineering

A terpyridine-modified chrysene derivative as an electron transporter to improve lifetime in phosphorescent OLEDs

Tsukasa Owada[1], Hisahiro Sasabe*[1,2,3], Yoshihito Sukegawa[1], Taiki Watanabe[1], Tomohiro Maruyama[1], Yuichiro Watanabe[1,2,3], Daisuke Yokoyama[1,2], Junji Kido*[1,2,3]

[1]Department of Organic Materials Science, Graduate School of Organic Materials Science, Yamagata University, 4-3-16 Jonan, Yonezawa, Yamagata 992-8510, Japan, [2]Research Center for Organic Electronics (ROEL), Yamagata University, 4-3-16 Jonan, Yonezawa, Yamagata 992-8510, Japan, [3]Frontier Center for Organic Materials (FROM), Yamagata University, 4-3-16 Jonan, Yonezawa, Yamagata 992-8510, Japan

E-mail: h-sasabe@yz.yamagata-u.ac.jp, kid@yz.yamagata-u.ac.jp

Keywords: organic light-emitting device; electron-transport; terpyridine; chrysene; phosphorescence

Abstract

In this work, we designed and developed a terpyridine-modified chrysene derivative, abbreviated as **B3TPyC**, to be used as electron-transport layers (ETLs) toward the construction of highly stable phosphorescent OLEDs. A green phosphorescent OLED with a **B3TPyC** ETL exhibited a low turn-on voltage of 2.4 V at 1 cd m^{-2} and an external quantum efficiency of 17.5% at 1000 cd m^{-2} with a long operation lifetime at 50% of the initial luminance (LT_{50}) of over 258 h at current density: 25 mA cm^{-2} (the initial luminance of approximately 12,000 cd m^{-2}), which corresponds to a LT_{50} of 19,000 h at 1000 cd m^{-2}. This is more than 1.5 times longer than the time of luminance decay provided by the phenylpyridine counterpart named **B3PyPC**. These results clearly show the potential and usefulness of terpyridine-based chrysene derivative to be applied in high-performance OLEDs with high operational stability.

1. Introduction

High-performance organic light-emitting devices (OLEDs) are absolutely imperative as energy-saving light sources for general lighting and in flat panel display applications.[1] In general, high-performance OLEDs consist of three primary layers: the hole transport layer (HTL), the emission layer (EML), and the electron transport layer (ETL).[2] Among these layers, the ETL plays a key role in determining the overall OLED performance and defines its final driving voltage, efficiency, and operational lifetime, evaluated as the operational lifetime at 50% of the initial luminance (LT_{50}). Organic semiconductor materials for ETLs typically comprise electron-deficient aromatic compounds such as triazine, pyrimidine, pyridine, and phenanthroline derivatives.[3] Among these materials, terpyridine derivatives are known to show excellent OLED performances and long lifetimes.[4] For example, Xiao and co-workers developed a terpyridine end-capped spirobifluorene derivative named 27-TPSF and constructed high-efficiency and long-lifetime green phosphorescent OLEDs based on tris[2-(p-tolyl)pyridine]iridium(III) [$Ir(mppy)_3$], with a maximum external quantum efficiency (η_{ext}) of 22.5% and a remarkable lifetime, with LT_{50} = 121 h at 10,000 cd m^{-2}, which is approximately three times longer than that of devices using a conventional ETL, 1,3,5-tris(1-phenyl-1H-benzimidazol-2-yl)benzene (TPBi).[4b,c] Sasabe and Kido have developed an oligopyridine-based high-performance ETL (6,6'-BPy3TPy) end-capped with terpyridine moieties, which allowed the realization of long-life, deep-red phosphorescent OLEDs based on bis(2,3-diphenylquinoxaline)iridium(dipivaloylmethane) [$(DPQ)_2Ir(dpm)$] with an η_{ext} of 15.3% and LT_{50} = 1680 h at 400 cd m^{-2} (at the current density of 2.5 mA cm^{-2}), which is longer than that of the device using 1,4-di(1,10-phenanthrorin-2-yl)benzene (DPB).[4d] Very recently, Sasabe and Kido also reported a chrysene-based phenylpyridine derivative named **B4PyPC**, which yielded high-efficiency and long-life green phosphorescent OLEDs based on tris(2-phenylpyridinato)iridium(III) [$Ir(ppy)_3$] with an η_{ext} of 17.8% and a long LT_{50} = 268 h at 11,170 cd m^{-2} (at the current density of 25 mA cm^{-2}), superior to the results of ETL based on the

anthracene/imidazole conjugate molecule, ZADN.[5] In this regard, a combination of terpyridine moieties and chrysene derivatives is a very intriguing option for the development of high-performance phosphorescent OLEDs with long lifetimes. In this work, we designed and developed a novel terpyridine-modified chrysene derivative named **B3TPyC** and used as ETL materials. The OLEDs employing **B3TPyC** exhibited an η_{ext} of 17.5% at 1000 cd m^{-2} with LT_{50} of over 258 h at the initial luminance of approximately 10,000 cd m^{-2} (current density: 25 mA cm^{-2}), which corresponds to LT_{50} of 19,000 h at 1000 cd m^{-2}. This is more than 1.5 times longer than that of the phenylpyridine counterpart named **B3PyPC**. These results clearly show the advantages of terpyridine-modified chrysene derivative as an ETL material for high-performance, long lifetime OLEDs.

2. Results and Discussion

2.1 DFT calculation

To improve the thermal and electrical stability of phenylpyridine-based ETLs, we recently found that a flat and rigid polycyclic aromatic hydrocarbon (PAH), chrysene, could be used as a promising core skeleton to construct ETLs.[5] Here, in addition, we installed two different types of terpyridine moieties as end-cap groups into the 6 and 12 positions of the chrysene skeleton to realize structures with superior stabilities, enhanced electron injection abilities, and better electron mobilities, which are caused by planarity induced by terpyridine moieties, and by a network of multiple intermolecular weak C-H···N hydrogen bonds.[6] Density functional theory (DFT) calculations of **B3TPyC** were performed by Gaussian09[7] to estimate the optoelectronic properties of the materials, such as the energies of the highest occupied molecular orbitals (HOMOs), the lowest unoccupied molecular orbitals (LUMOs), and the excited singlet and triplet states (E_S and E_T). The optimized ground-state structures were calculated at the RB3LYP 6-31G (d) level, and single-point energies were calculated at the corresponding RB3LYP 6-311+G (d, p) levels. Here, we also showed the calculation results of

the phenylpyridine counterpart **B3PyPC** as a reference. The results are shown in **Figure 1(a)** and **Table 1**. Similar electron cloud distributions of HOMOs and LUMOs were observed in **B3TPyC**: HOMO showed a more significant electron density over the chrysene moiety irrespective of the peripheral pyridine rings, while LUMO showed bigger distributions on the atoms of the 2,6-dipyridylchrysene moiety. For a HOMO and LUMO pair, the energies were successively lower in the order of **B3PyPC** > **B3TPyC**, influenced by the electron-withdrawing ability of the peripheral pyridine rings. The terpyridine derivatives showed much deeper LUMO energies compared with those of the phenylpyridine derivative. Thus, superior electron injection abilities leading to low drive voltages in OLEDs were expected from **B3TPyC** compared with those of the phenylpyridine counterpart **B3PyPC**. All the E_Ts were calculated to be lower than 2.35 eV, which is attributed to the chrysene core skeleton.[5,8]

2.2 Synthesis and Thermal Properties

The target compounds were easily prepared via a two-step reaction comprising a Suzuki–Miyaura coupling reaction from 6,12-dibromochrysene as a starting material (**Scheme S1**). The target compound **B3TPyC** was characterized using ^{1}H-NMR, mass spectroscopy, and elemental analysis. The thermal properties, such as the 5% weight loss temperature (T_{d5}), glass transition temperature (T_g), and melting point (T_m), were evaluated using thermogravimetric analysis (TGA) and differential scanning calorimetry (DSC). High T_ms were observed at over 380 °C, and high T_{d5}s were observed at around 500 °C. These values indicate the high thermal stability of **B3TPyC**, attributable to the flat and rigid chemical structure of the chrysene skeleton. None of the compounds had T_g between 50 and 430 °C. Then, we investigated the optoelectronic properties of vacuum-deposited thin films of these materials. The UV-Vis absorption spectrum of the vacuum-deposited film of **B3TPyC** is presented in **Fig. 1(b)**. This film exhibits a strong absorption peak at 346 nm, derived from the chrysene skeleton. The optical bandgap (E_g) was estimated to be 3.1 eV on the basis of the UV-Vis absorption edge.

The PL spectrum is shown in **Fig. 1(c)**. Terpyridine-based **B3TPyC** showed silightly longer peak wavelength compared with **B3PyPC** presumably due to the expanded π-conjugation induced by the planarization effect of terpyridine groups. The ionization potential (I_p) was measured by photoelectron yield spectroscopy (PYS). The I_p decreased in the order of **B3PyPC** (–6.0 eV) > **B3TPyC** (–6.1 eV) as predicted from DFT calculations. Compared with that of phenylpyridine-based **B3PyPC**, terpyridine-based **B3TPyC** show deeper I_p value, most likely due to the stronger electron-withdrawing ability of their terpyridine end-capping moieties. The electron affinity (E_a) showed a similar trend and was estimated from the E_g and I_p values to be –2.8 eV for **B3PyPC**, and –3.2 eV for **B3TPyC**. Therefore, we can expect superior electron injection ability of terpyridine derivative **B3TPyC** as compared with those of phenylpyridine-based **B3PyPC**. All the physical properties of **B3TPyC** are summarized in **Table 1**.

2.3 Surface Morphology and Molecular Orientation

The surface roughness of 100 nm-thick films deposited onto indium-tin-oxide (ITO) was observed using a tapping mode atomic force microscope (AFM). All the films of **B3PyPC** and **B3TPyC** exhibited a root mean square (rms) roughness (R_{rms}) of less than 1 nm, which allows them to produce optimal optoelectronic devices by vacuum deposition (**Fig. 2**). Note that we were not able to observe the crystallization of the vacuum-deposited films in a week, and no crystallization was observed even after the deposition of Al metal cathode.

Then, we further investigated the molecular aggregation behavior in the deposited films using variable-angle spectroscopic ellipsometry (VASE).[9] We found that both films produced large optical anisotropies of the refractive indices and extinction coefficients, which mean highly horizontally oriented films. In particular, terpyridine-based **B3TPyC** qualitatively gave larger anisotropies of refractive indices than did phenylpyridine-based **B3PyPC** (**Fig. 3**). This is most likely due to the planarization effect of end-capping moieties induced by intra-molecular C-H···N hydrogen bonds in terpyridines.[6] Similar trends, showing that the planarization effect

can yield superior horizontal orientation, have already been reported using bis-terpyridine derivatives **n-TerPyB**.[4a] Note that we did not quantify the order parameter S, because the peaks at around 350 nm were not large enough for a reliable evaluation. Further, compared with case when methylpyrimidine-based (**BnPyMPM**) derivatives[6a,b] are used, the contributions of weak hydrogen bonds involving the peripheral pyridine rings to the horizontal orientation seem to be relatively small, most likely due to the much larger contribution of π-π interactions from the chrysene skeleton.

2.4 OLED performances

We fabricated tris(2-phenylpyridinato)iridium(III) [$Ir(ppy)_3$]-based OLEDs to verify the performances of **B3TPyC** as an ETL. The device structure was [ITO (130 nm) / triphenylamine containing polymer: 4-isopropyl-4'-methyldiphenyl-iodoniumtetrakis(pentafluorophenyl)borate (PPBI)[10] (20 nm) / *N,N'*-di(1-naphthyl)-*N,N'*-(1,1'-biphenyl)-4,4'-diamine (NPD) (20 nm) / $Ir(ppy)_3$ 12 wt% doped 3,3-di(9H-carbazol-9-yl)biphenyl (mCBP) (15 nm)[11] / 2-(3'-(dibenzo[*b,d*]thiophen-4-yl)-[1,1'-biphenyl]-3-yl)-4,6-diphenyl-1,3,5-triazine (DBT-TRZ)[12] (10 nm) / (8-quinolinolato) lithium (Liq) 20 wt% doped-ETL (40 nm)/Liq (1 nm)/Al (100 nm)]. All the materials used in these OLEDs are shown in **Fig. 4(a)**, and energy diagram is depicted in **Fig. 4(b)**. In this device architecture, we used the exciton- and hole-blocking layer DBT-TRZ (E_T = 2.90 eV)[12] between the emission layer and ETL to prevent the quenching of the triplet excitons of $Ir(ppy)_3$. Further, we used Liq doped-ETL for improved electron-injection and lifetime.[1f, 13] Current density–voltage and luminance–voltage (J–V and L–V) characteristics are displayed in **Fig. 4(c)** and **4(d)**, respectively. The turn-on voltage at 1 cd m^{-2} was recorded to be 2.42 V for **B3TPyC** and 2.51 V for **B3PyPC**. Apparently, terpyridine-based **B3TPyC** derivatives gave lower operating voltages due to the deeper E_a. The maximum η_{ext}s were recorded to be 18.7% for **B3TPyC** and

20.3% for **B3PyPC** (**Fig. 4(e)**). Although phenylpyridine-based **B3PyPC** gave a lower current density compared with terpyridine-based **B3TPyC**, it exhibited slightly better η_{ext}s due to the superior carrier balance. The operating voltage at 1000 cd m^{-2} was recorded to be 3.46 V for **B3TPyC** and 3.61 V for **B3PyPC**. Owing to the low operating voltage, **B3TPyC**-based devices exhibited high power efficiencies of over 60 lm W^{-1} with η_{ext} of 18%. Finally, we evaluated the devices' stabilities at the constant current density of 25 mA cm^{-2}, which corresponds approximately to an initial luminance of 11,000 cd m^{-2} (**Fig. 4(f)**). From these measurements, terpyridine-based **B3TPyC** devices showed the best stability with a LT_{50} of over 258 h, which was more than 1.5 times longer than for those employing phenylpyridine-based **B3PyPC**. This value for the lifetime at 11,000 cd m^{-2} corresponds to a LT_{50} of approximately 19,000 h at 1000 cd m^{-2}.[14] As such, this terpyridine-based **B3TPyC** is clearly promising ETL materials for low operating voltage OLEDs, providing high stability. Further, we fabricated electron only devices using these ETLs to qualitatively evaluate the electron-transport properties (**Figure S5)**. Consequently, the order of current density was **B3PyPC** > **B3TPyC**, and the tendency was same in that of OLEDs shown in **Figure 4(c)**. Among terpyridine-based ETLs, the higher electron-transport properties led to the shorter lifetime in OLEDs.

3. Conclusion

We successfully developed a terpyridine-modified chrysene derivative **B3TPyC**, and investigated their optoelectronic properties as ETLs in phosphorescent OLEDs. We showed that **B3TPyC** can be easily prepared via a two-step reaction from commercially available 6,12-dibromochrysene as a starting material, and that they exhibit excellent thermal stabilities thanks to the structural characteristics of the chrysene skeleton and high electron injection abilities caused by the terpyridine end-cap groups, which are more promising moieties than phenylpyridine end-cap groups. An AFM study showed **B3TPyC** formed very smooth films via a vacuum deposition technique, with a Rrms of less than 1.0 nm. VASE analyses revealed

that terpyridine groups clearly allow a superior horizontal orientation of the transition dipole moments. Finally, we successfully fabricated green phosphorescent OLEDs based on $Ir(ppy)_3$ using **B3TPyC** as the ETLs. The OLED with **B3TPyC** exhibited a low turn-on voltage of 2.4 V, $\eta_{ext,100}$ over 18%, $\eta_{p,100}$ over 60 lm W^{-1}, and a LT_{50} of approximately 19,000 at 1000 cd m^{-2}, which was more than 1.5 times longer than that of the device with phenylpyridine-based **B3PyPC**. Although these data are preliminary results combined with well-known commercially available materials such as NPD, $Ir(ppy)_3$, mCBP, and DBT-TRZ, however, we can clearly show the advantages of terpyridine-based chrysene derivatives compared with those of bipyridylphenyl derivatives, such as deeper E_a to enhance electron-injection leading to lower driving voltages, superior horizontal orientation potentially leading to high carrier mobility, and enhanced device stability. This approach is very informative, and reproducible in the scientific community. Unfortunately, the reason why terpyridine-modified chrysene derivatives showed better device stability compared with that of bipyridylphenyl derivatives is not clear at this stage. We believe that these results clearly show the potential and utility of terpyridine-based chrysene derivatives as ETLs for high-performance OLEDs with high operational stability.

Acknowledgements

We gratefully acknowledge the partial financial support from the Center of Innovation (COI) Program from the Japan Science and Technology Agency, JST. H.S. acknowledges financial support in part by JSPS KAKENHI (17H03131) from JSPS.

References

1 (a) J. Kido, M. Kimura, K. Nagai, *Science* **1995**, *267*, 1332; (b) Y. Sun, N. C. Giebink, H. Kanno, B. Ma, M. E. Thompson, S. R. Forrest, *Nature* **2006**, *440*, 908; (c) B. W. D'Andrate, J. Esler, C. Lin, V. Adamovich, S. Xia, M. S. Weaver, R. Kwong, J. J. Brown, *Proc. SPIE* **2008**, *7051*, 70510Q–1; (d) S. Reineke, F. Lindner, G. Schwartz, N. Seidler, K. Walzer, B. Lussem, K. Leo, *Nature* **2009**, *459*, 234; (e) K. Walzer, B. Maennig, M. Pfeiffer, K. Leo, *Chem. Rev.* **2007**, *107*, 1233; (f) H. Sasabe, J. Kido, *J. Mater. Chem. C* **2013**, *1*, 1699.

2 C. Adachi, T. Tsutsui, S. Saito, *Appl. Phys. Lett.* **1990**, *57*, 531.

3 (a) A. P. Kulkarni, C. J. Tonzola, A. Babel and S. A. Jenekhe, *Chem. Mater.* **2004**, *16*, 4556; (b) G. Hughes and M. R. Bryce, *J. Mater. Chem.* **2005**, *15*, 94; (c) H. Sasabe, J. Kido, *Chem. Mater.* **2011**, ***23***, 621; (d) L. Xiao, Z. Chen, B. Qu, J. Luo, S. Kong, Q. Gong, J. Kido, *Adv. Mater.* **2011**, *23*, 926; (e) D. Chen, S. -J. Su, Y. Cao, *J. Mater. Chem. C*, **2014**, *2*, 9565–9578.

4 (a) Y. Watanabe, R. Yoshioka, H. Sasabe, T. Kamata, H. Katagiri, D. Yokoyama, J. Kido, *J. Mater. Chem. C*, **2016**, 4, 8980; (b) M. Bian, D. Zhang, Y. Wang, Y-H. Chung, Y. Liu, H. Ting, L. Duan, Z. Chen, Z. Bian, Z. Liu, L. Xiao, *Adv. Funct. Mater.* **2018,** 28, 1800429; (c) X. Guo, M. Bian, F. Lv, Y. Wang, Z. Zhao, Z. Bian, Z. Liu, B. Qu, L. Xiao, Z. Chen, *J. Mater. Chem. C*, **2019**, *10*, 1039; (d) Y. Watanabe, D. Yokoyama, T. Koganezawa, H. Katagiri, T. Ito, S. Ohisa, C. Takayuki, H. Sasabe, J. Kido, *Adv. Mater.* **2019,** 31, 1808300.

5 T. Watanabe, H. Sasabe, T. Owada, T. Maruyama, Y. Watanabe, H. Katagiri, J. Kido, *Chem Lett.* **2019**, *48*, 457.

6 (a) H. Sasabe, D. Tanaka, D. Yokoyama, T. Chiba, Y.-J. Pu, K.-i. Nakayama, M. Yokoyama, J. Kido, *Adv. Funct. Mater.* **2011**, *21*, 336; (b) D. Yokoyama, H. Sasabe, Y. Furukawa, C. Adachi, J. Kido, *Adv. Funct. Mater.* **2011**, *21*, 1375; (c) Y. Watanabe, H. Sasabe, D. Yokoyama, T. Beppu, H. Katagiri, Y.-J. Pu, J. Kido, *Adv. Opt. Mater.* **2015**, *3*,

769; (d) T. Kamata, H. Sasabe, Y. Watanabe, D. Yokoyama, H. Katagiri, J. Kido, *J. Mater. Chem. C* **2016**, *4*, 1104; (e) Y. Watanabe, H. Sasabe, D. Yokoyama, T. Beppu, H. Katagiri, J. Kido, *J. Mater. Chem. C* **2016**, *4*, 3699.

7 *Gaussian 09*, Revision D.01, M. J. Frisch, G. W. Trucks, H. B. Schlegel, G. E. Scuseria, M. A. Robb, J. R. Cheeseman, G. Scalmani, V. Barone, B. Mennucci, G. A. Petersson, H. Nakatsuji, M. Caricato, X. Li, H. P. Hratchian, A. F. Izmaylov, J. Bloino, G. Zheng, J. L. Sonnenberg, M. Hada, M. Ehara, K. Toyota, R. Fukuda, J. Hasegawa, M. Ishida, T. Nakajima, Y. Honda, O. Kitao, H. Nakai, T. Vreven, J. A. Montgomery, Jr., J. E. Peralta, F. Ogliaro, M. Bearpark, J. J. Heyd, E. Brothers, K. N. Kudin, V. N. Staroverov, R. Kobayashi, J. Normand, K. Raghavachari, A. Rendell, J. C. Burant, S. S. Iyengar, J. Tomasi, M. Cossi, N. Rega, J. M. Millam, M. Klene, J. E. Knox, J. B. Cross, V. Bakken, C. Adamo, J. Jaramillo, R. Gomperts, R. E. Stratmann, O. Yazyev, A. J. Austin, R. Cammi, C. Pomelli, J. W. Ochterski, R. L. Martin, K. Morokuma, V. G. Zakrzewski, G. A. Voth, P. Salvador, J. J. Dannenberg, S. Dapprich, A. D. Daniels, Ö. Farkas, J. B. Foresman, J. V. Ortiz, J. Cioslowski, and D. J. Fox, Gaussian, Inc., Wallingford CT, 2013.

8 D. D. Morgan, D. Warshawsky, T. Atkinson, *Photochem. Photobiol.* **1977**, *25*, 31.

9 D. Yokoyama, *J. Mater. Chem.* **2011**, *21*, 19187.

10 J. Kido, G. Harada, M. Komada, H. Shionoya, K. Nagai, *ACS. Synp. Ser.* **1997**, *672*, 381.

11 P. Shrögel, N. Langer, C. Shildknecht, G. Wagenblast, C. Lennartz, P. Strohriegl, *Org. Electron.* **2011**, *12*, 2047.

12 (a) Y. Nagai, H. Sasabe, J. Takahashi, N. Onuma, T. Ito, S. Ohisa, J. Kido, *J. Mater. Chem. C* **2017**, *5*, 527; (b) T. Ito, H. Sasabe, Y. Nagai, Y. Watanabe, N. Onuma, J. Kido, *Chem. Eur. J.* **2019**, *25*, 7308.

13 H. Sasabe, K. Minamoto, Y.-J. Pu, M. Hirasawa, J. Kido, *Org. Electron.* **2012**, *13*, 2615.

14 D. Zhang, M. Cai, Y. Zhang, D. Zhang, L. Duan, *Mater. Horiz.* **2016**, 3, 145.

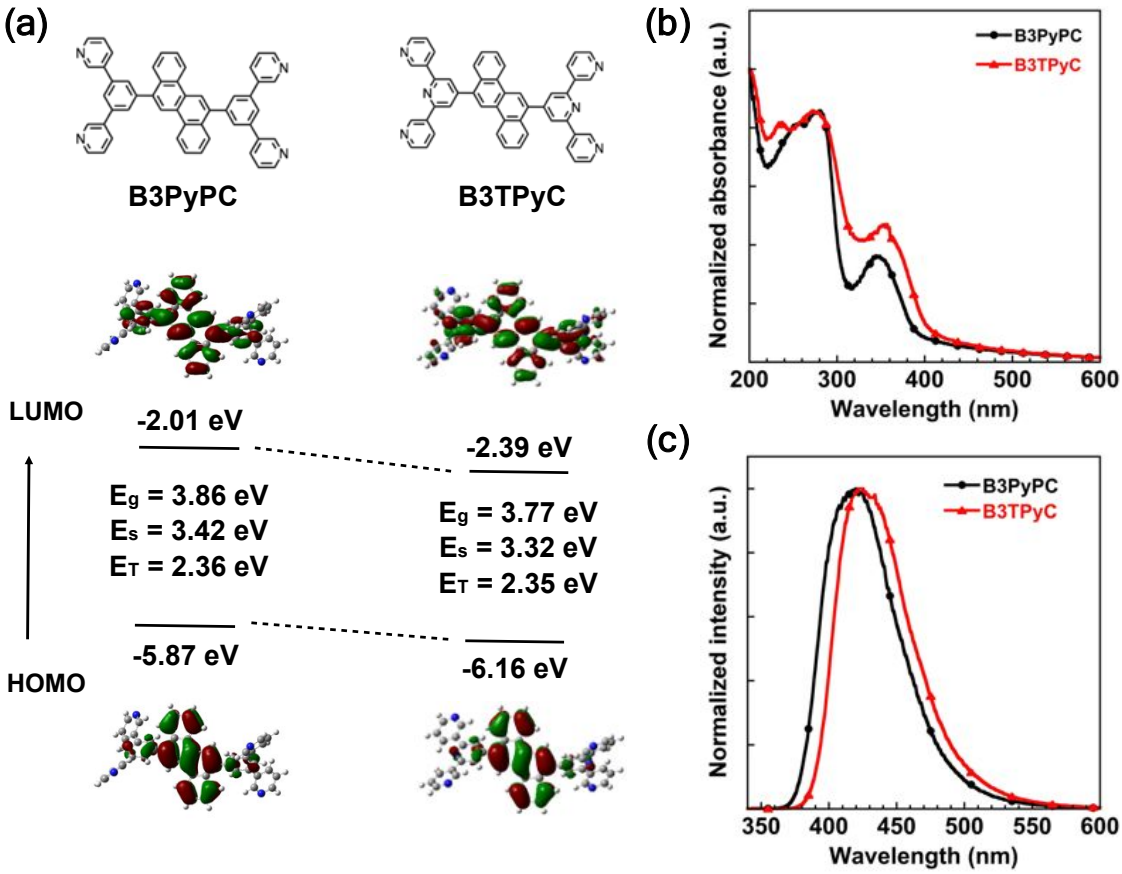

Fig. 1 (a) Molecular structures and the results of DFT calculations of **B3PyPC** and **B3TPyC**. (b) UV-vis absorption spectra, and (c) PL spectra of **B3PyPC** and **B3TPyC** vacuum-deposited films.

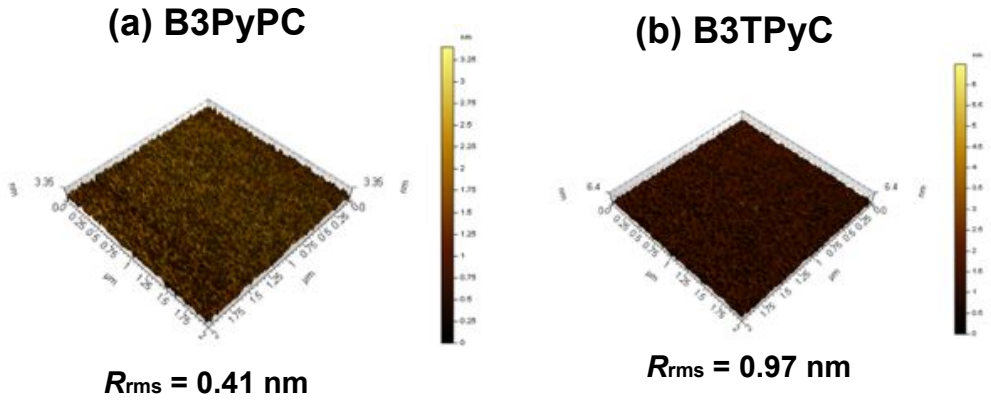

Fig. 2 AFM images and R_{rms} values of 100 nm-thick films of (a) **B3PyPC** and (b) **B3TPyC** vacuum-deposited films.

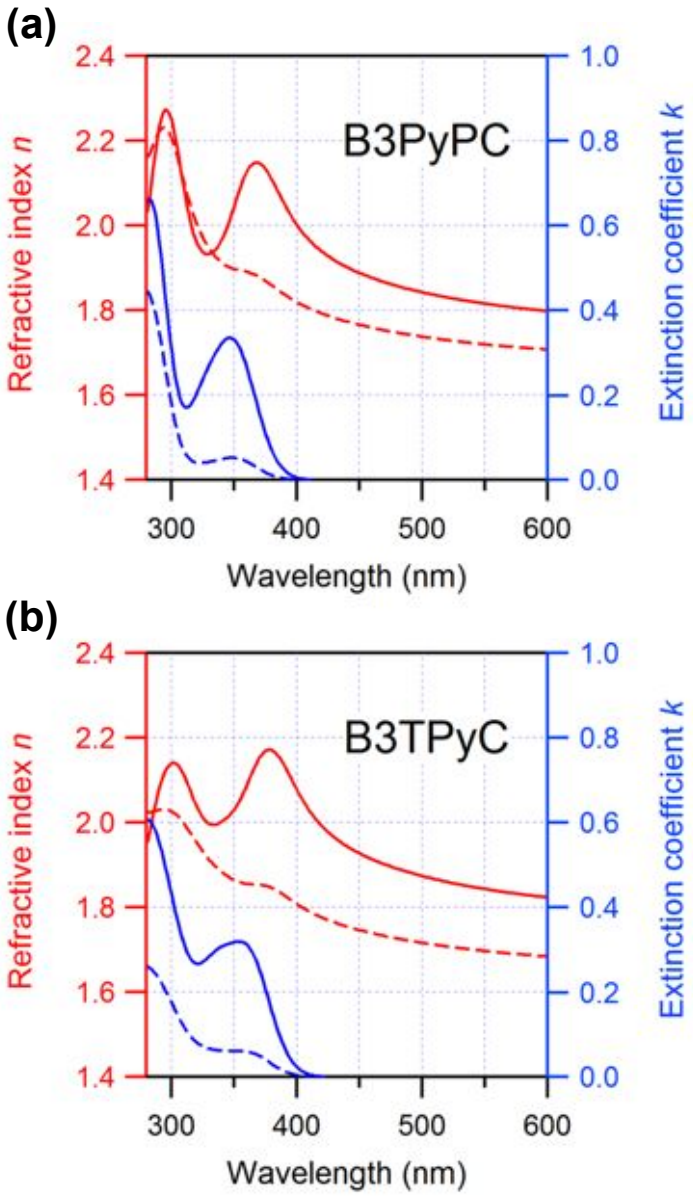

Fig. 3 Anisotropies of the refractive indices and extinction coefficients of (a) **B3PyPC** (b) **B3TPyC** vacuum deposited films. The solid and broken lines indicate the horizontal and vertical components of the optical constants, respectively.

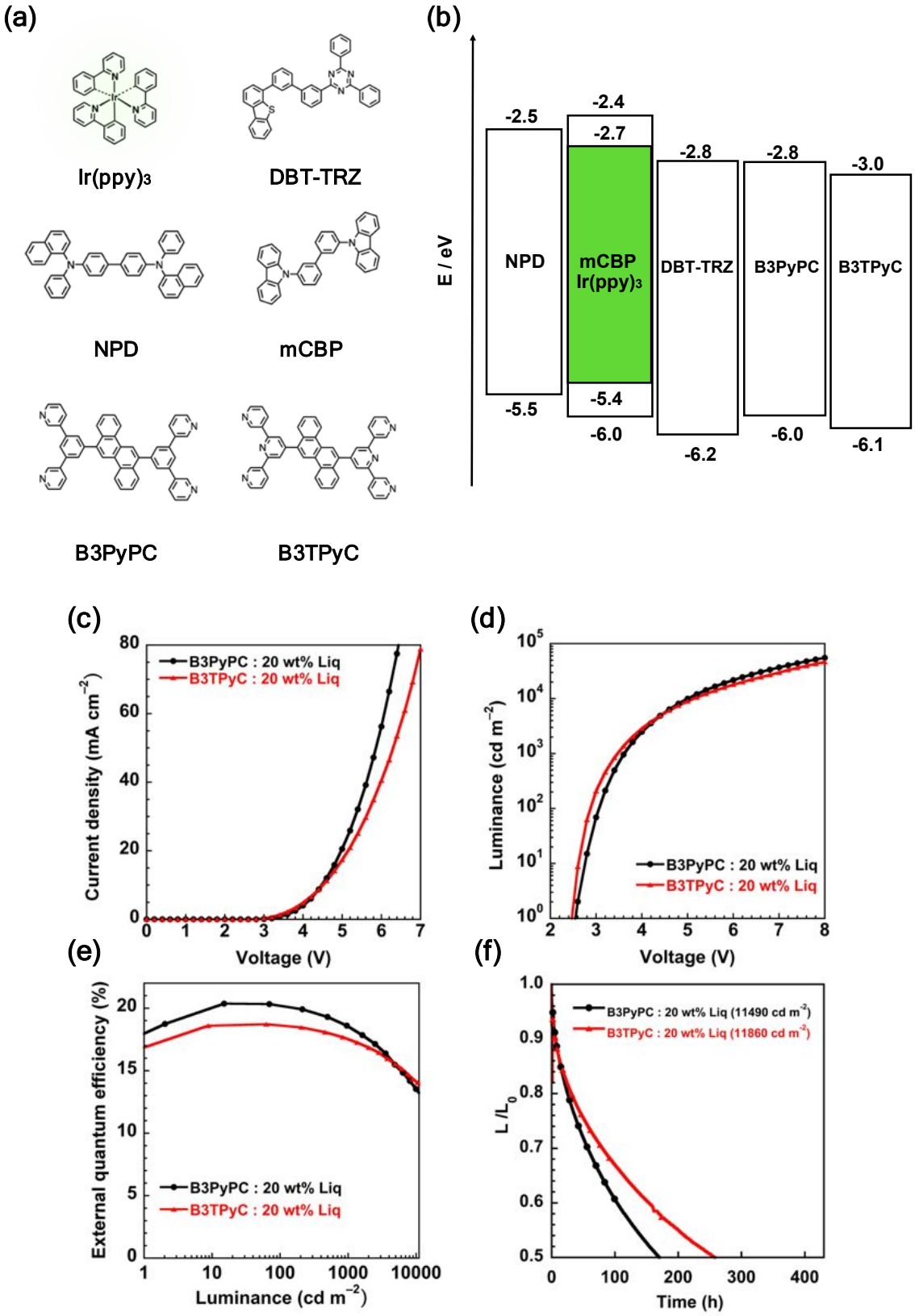

Fig. 4 (a) Chemical structures and (b) energy diagram of the fabricated devices. The device performance of the green OLEDs; (c) current density–voltage characteristics; (d) luminance–voltage characteristics; (e) external quantum efficiency–luminance characteristics; and (f) normalized luminance as a function of operation time at the initial current density of 25 mA cm^{-2} for the devices employing either **B3PyPC** or **B3TPyC** as the ETL.

Table 1. Properties of **BnTPyC**s derivatives.

Compound	Mw	T_g[a]/T_m[a]/T_{d5}[b] (°C)	HOMO[c]/LUMO[c]/ΔE_{H-L}[d] (eV)	I_p[e]/E_g[f]/E_a[g] (eV)
B3TPyC	690	n.d./381/501	–6.16/–2.39/3.77	–6.1/3.1/–3.0
B3PyPC	688	n.d./390/499	–5.87/–2.01/3.86	–6.0/3.2/–2.8

[a]T_g and T_m were determined using DSC. [b]T_{d5} was determined using TGA. [c]HOMO and LUMO were calculated at the RB3LYP 6-311+G(d,p)/RB3LYP 6-31G(d) level. [d]ΔE_{H-L} = HOMO–LUMO. [e]I_p was determined using PYS. [f]E_g was taken as the point where the normalized absorption spectra intersected. [g]E_a was calculated using I_p and E_g.

Table 2. Summary of OLED performances.

ETL	V_{on}[a] (V)	$V_{100}/\eta_{c,100}/\eta_{p,100}/\eta_{ext,100}$[b] (V/cd A^{-1}/lm W^{-1}/%)	$V_{1000}/\eta_{c,1000}/\eta_{p,1000}/\eta_{ext,1000}$[c] (V/cd A^{-1}/lm W^{-1}/%)	LT_{50}[d] (h) @25 mA cm^{-2}	LT_{50}[e] (h) @1000 cd m^{-2}
B3TPyC	2.42	2.85/74.2/67.3/18.7	3.46/57.4/63.3/17.5	258	≈ 19000
B3PyPC[5]	2.51	3.04/75.3/72.9/20.2	3.61/58.1/66.8/18.6	170	≈ 12000
DPB	2.43	2.88/76.1/69.5/19.3	3.43/54.9/59.9/16.6	243	≈ 11000

[a]Turn-on voltage at 1 cd m^{-2}. [b]Voltage, current efficiency (η_c), power efficiency (η_p), and external quantum efficiency (η_{ext}) at 100 cd m^{-2}. [c]Voltage, η_c, η_p, and η_{ext} at 1,000 cd m^{-2}. [d]Operation lifetime at 50% of the initial luminance of approximately 11000 cd m^{-2} (current density : 25 mA cm^{-2}) [e]Operation lifetime at 50% of the initial luminance of approximately 1000 cd m^{-2} estimated using the well known stretched exponential decay function.[13]

Graphical Abstract

A terpyridine-modified chrysene derivative as an electron transporter to improve lifetime in phosphorescent OLEDs

Tsukasa Owada, Hisahiro Sasabe*, Yoshihito Sukegawa, Taiki Watanabe, Tomohiro Maruyama, Yuichiro Watanabe, Daisuke Yokoyama, Junji Kido*

A terpyridine-end-capped chrysene shows superior electron-transport ability with high operation stability in organic light-emitting devices (OLEDs). A green phosphorescent OLED exhibited a low turn-on voltage of 2.4 V at 1 cd m^{-2} and an external quantum efficiency of 17.5% at 1000 cd m^{-2} with a long operation lifetime at 50% of the initial luminance (LT_{50}) of 19,000 h at 1000 cd m^{-2}.